Self-Assembly Organometallic Squares with Terpyridyl Metal Complexes as Bridging Ligands

Shih-Sheng Sun and Alistair J. Lees*

Department of Chemistry, State University of New York at Binghamton, Binghamton, New York 13902-6016

Received February 8, 2001

A series of novel heterometallic square complexes with the general molecular formulas {*fac*-Br(CO)$_3$Re[μ-(pyterpy)$_2$M]}$_4$(PF$_6$)$_8$ and {(dppf)Pd[μ-(pyterpy)$_2$Ru]}$_4$(PF$_6$)$_8$(OTf$_8$ (**4**), where M = Fe (**1**), Ru (**2**), or Os (**3**), pyterpy is 4′-(4‴-pyridyl)-2,2′:6′,2″-terpyridine, dppf = 1,1′-bis(diphenylphosphino)ferrocene and OTf is trifluoromethanesulfonate, were prepared by self-assembly between BrRe(CO)$_5$ or (dppf)Pd(H$_2$O)$_2$(OTf)$_2$ and (pyterpy)$_2$M(PF$_6$)$_2$. The obtained NMR spectra, IR spectra, electrospray ionization mass spectra, and elemental analyses are all consistent with the proposed square structures incorporating terpyridyl metal complexes as bridging ligands. Multiple redox processes were observed in all square complexes. All four complexes display strong visible absorptions in the region 400−600 nm, which are assigned as metal (Fe, Ru, or Os)-to-ligand (pyterpy) charge transfer (MLCT) bands. Square **3** exhibits an additional weak band at 676 nm, which is assigned to an Os-based ^{3}MLCT band. For each complex, the bands centered between 279 and 377 nm are assigned as pyterpy-based $\pi-\pi^*$ bands and the Re-based MLCT band. Square **3** is luminescent in room-temperature solution, while squares **1**, **2**, and **4** do not have any detectable luminescence under identical experimental conditions.

Introduction

Luminescent polynuclear transition-metal complexes containing multichromophroic ligands with extended conjugation have been extensively studied in recent years, possibly due to their potential use as sensors, probes, and photonic devices.[1] Among the numerous luminescent transition-metal complexes, Re(I)-, Ru(II)-, and Os(II)-based polypyridyl chromophores are the most commonly studied because they usually exhibit fairly strong luminescence in the visible region and the photophysical properties are relatively easily tuned by simply modifying the coordinated or ancillary ligands. These compounds also have the advantage of being relatively stable with respect to photodecomposition. In each case, the emission from the complexes usually originates from triplet metal-to-ligand charge transfer (^{3}MLCT) excited state(s) and has the added feature of being typically sensitive to the nature of the environment and influenced by solvent, temperature, and pH.[2]

Recently, we have been interested in transition-metal based macrocyclic complexes which are self-assembled from different predesigned, structural information coded building blocks.[3] The relatively weak metal−ligand interactions allow the systems to reversibly perform structural error checking until the most thermodynamically stable products are reached. Our previous studies have indicated that the geometries and physical properties of such self-assembly macrocyclic complexes are highly dependent on the bridging ligands.[4] Moreover, transition-metal based macrocyclic complexes have shown the potential for being used as hosts for a variety of guest molecules, from anions to small organic molecules,[5−8] and subsequent recognition events can be conveniently monitored by optical,[4c,5] NMR,[4d,6] mass spectrometry,[7] or electrochemical techniques.[8] Since the first

* To whom correspondence should be addressed. E-mail: alees@binghamton.edu.

(1) (a) Sauvage, J.-P.; Collin, J.-C.; Chambron, S.; Guillerez, C.; Coudret, V.; Balzani, V.; Barigelletti, F.; De Cola, L.; Flamigni, L. *Chem. Rev.* **1994**, *94*, 993. (b) Balzani, V.; Juris, A.; Venturi, M.; Campagna, S.; Serroni, S. *Chem. Rev.* **1996**, *96*, 759.

(2) (a) Lees, A. J. *Chem. Rev.* **1987**, *87*, 711. (b) *Supramolecular Photochemistry*; Balzani, V., Scandola, F., Eds; Ellis Horwood: Chichester, U.K., 1991.

(3) (a) Leininger, S.; Olenyuk, B.; Stang, P. J. *Chem. Rev.* **2000**, *100*, 853 and references therein. (b) Swiegers, G. F.; Malefetse, T. J. *Chem. Rev.* **2000**, *100*, 3483 and references therein.

(4) (a) Sun, S.-S.; Lees, A. J. *Inorg. Chem.* **1999**, *38*, 4181. (b) Sun, S.-S.; Silva, A. S.; Brinn, I. M.; Lees, A. J. *Inorg. Chem.* **2000**, *39*, 1344. (c) Sun, S.-S.; Lees, A. J. *J. Am. Chem. Soc.* **2000**, *122*, 8956. (d) Sun, S.-S.; Lees, A. J. *Chem. Commun.* **2001**, 103.

(5) Some selective examples: (a) Ikeda, A.; Ayabe, M.; Shinkai, S.; Sakamoto, S.; Yamaguchi, K. *Org. Lett.* **2000**, *2*, 3707. (b) Xu, D.; Hong, B. *Angew. Chem., Int. Ed.* **2000**, *39*, 1826. (c) Xu, D.; Murfee, H. J.; van der Veer, W. E.; Hong, B. *J. Organomet. Chem.* **2000**, *596*, 53. (d) Slone, R. V.; Hupp, J. T. *Inorg. Chem.* **1997**, *36*, 5422. (e) Slone, R. V.; Yoon, D. I.; Calhoun, R. M.; Hupp, J. T. *J. Am. Chem. Soc.* **1995**, *117*, 11813.

(6) Some selective examples: (a) Schnebeck, R.-D.; Freisinger, E.; Glahe, F.; Lippert, B. *J. Am. Chem. Soc.* **2000**, *122*, 1381. (b) Hiraoka, S.; Kubota, Y.; Fujita, M. *Chem. Commun.* **2000**, 1509. (c) Jeong, K.-S.; Cho, Y. L.; Chang, S.-Y.; Park, T.-Y.; Song, J. U. *J. Org. Chem.* **1999**, *64*, 9459. (d) Ma, G.; Jung, Y. S.; Chung, D. S.; Hong, J.-I. *Tetrahedron Lett.* **1999**, *40*, 531. (e) Jeong, K.-S.; Cho, Y. L.; Song, J. U.; Chang, H.-Y.; Choi, M.-G. *J. Am. Chem. Soc.* **1998**, *120*, 10982. (f) Fujita, M.; Nagao, S.; Iida, M.; Ogata, K.; Ogura, K. *J. Am. Chem. Soc.* **1993**, *115*, 1574. (g) Fujita, M.; Yazaki, J.; Ogura, K. *Tetrahedron Lett.* **1991**, *32*, 5589. (h) Maverick, A. W.; Buckingham, S. C.; Yao, Q.; Bradbury, J. R.; Stanley, G. G. *J. Am. Chem. Soc.* **1986**, *108*, 7430.

(7) Some selective examples: (a) Yoshizawa, M.; Kusukawa, T.; Fujita, M.; Yamaguchi, K. *J. Am. Chem. Soc.* **2000**, *122*, 6311. (b) Tashiro, K.; Aida, T.; Zheng, J.-Y.; Kinbara, K.; Saigo, K.; Sakamoto, S.; Yamaguchi, K. *J. Am. Chem. Soc.* **1999**, *121*, 9477. (c) Bakhtiar, R.; Chen, H.; Ogo, S.; Fish, R. H. *Chem. Commun.* **1997**, 2135.

(8) Some selective examples: (a) Benkstein, K. D.; Hupp, J. T.; Stern, C. L. *Angew. Chem., Int. Ed.* **2000**, *39*, 2891. (b) Keefe, M. H.; Slone, R. V.; Hupp, J. T.; Czaplewski, K. F.; Snurr, R. Q.; Stern, C. L. *Langmuir* **2000**, *16*, 3964. (c) Bélanger, S.; Hupp, J. T.; Stern, C. L.; Slone, R. V.; Watson, D. F.; Carrell, T. G. *J. Am. Chem. Soc.* **1999**, *121*, 557. (d) Bélanger, S.; Hupp, J. T. *Angew. Chem., Int. Ed.* **1999**, *38*, 2222.

10.1021/ic0101681 CCC: $20.00
Published on Web 05/15/2001

self-assembly molecular square, prepared by Fujita and co-workers in 1990 that is based on a labile Pd(II) complex,[9] many self-assembly molecular squares utilizing Pd(II) or Pt(II) as corners have been reported in the literature.[3] In 1995, Hupp and co-workers first introduced self-assembly molecular squares utilizing octahedral *fac*-tricarbonyl Re(I) halide as corners.[5e,10] The incorporation of potentially luminescent *fac*-tricarbonyl Re(I) diimine chromophores into the macrocyclic structures offers rich photophysical properties and potential applications in sensors or ultrafine sieves. Since then, numerous Re(I) carbonyl based macrocyclic complexes have appeared utilizing a variety of bridging ligands.[4,5d,8a,11] In this paper, we have utilized both the strategies of self-assembly and "complexes as ligands"[4b,12] and report the preparation of a series of octanuclear molecular squares with the general molecular formulas $\{fac\text{-}Br(CO)_3Re[\mu\text{-}(pyterpy)_2M]\}_4(PF_6)_8$ and $\{(dppf)Pd[\mu\text{-}(pyterpy)_2Ru]\}_4(PF_6)_8(OTf)_8$, where pyterpy is 4′-(4‴-pyridyl)-2,2′:6′,2″-terpyridine, dppf = 1,1′-bis(diphenylphosphino)ferrocene and M = Fe, Ru, or Os. The electrochemical and spectroscopic properties of these octanuclear molecular squares are also presented.

Experimental Section

Materials and General Procedures. All reactions and manipulations were carried out under nitrogen or argon with the use of standard inert-atmosphere and Schlenk techniques. Solvents used for synthesis were dried by standard procedures and stored under nitrogen.[13] Solvents used in luminescent and electrochemical studies were spectroscopic and anhydrous grade, respectively. The ligands and complexes 4′-(4‴-pyridyl)-2,2′:6′,2″-terpyridine (pyterpy),[14] $[Fe(pyterpy)_2][PF_6]_2$,[14] $[Ru(pyterpy)_2][PF_6]_2$,[15] $[Os(pyterpy)_2][PF_6]_2$,[15] and $(dppf)Pd(H_2O)_2(OTf)_2$[16] were prepared by literature methods. All other chemicals are commercially available. ^{1}H NMR spectra were obtained using either a Brücker AM 360 spectrometer or a Brücker AC 300 spectrometer, and ^{13}C, ^{31}P and ^{19}F NMR spectra were obtained using a Brücker AM 360 spectrometer. ^{1}H NMR spectra are reported in ppm relative to the proton resonance resulting from incomplete deuteration of the NMR solvent; ^{31}P NMR spectra are reported in ppm relative to external 85% H_3PO_4 at 0.00 ppm; and ^{19}F NMR spectra are reported in ppm relative to external $CFCl_3$ at 0.00 ppm. Infrared spectra were measured on a Nicolet 20SXC Fourier transform infrared spectrophotometer. Electrospray mass spectra were obtained using a Finnigan MAT TSQ700 triple quadrupole mass spectrometer equipped with a Finnigan electrospray interface. UV-vis spectra were obtained using an HP 8450A diode array spectrophotometer. Emission spectra were recorded in deoxygenated solvent solutions at 293 K, with an SLM 48000S lifetime fluorescence spectrophotometer equipped with a red sensitive Hamamatsu R928 photomultiplier tube. Reported luminescence quantum yields are relative to $Os(bpy)_3(PF_6)_2$ in CH_3CN ($\Phi_{em} = 0.005$), unless otherwise noted.[17,18] The detailed procedures for photophysical measurements have been described in an earlier paper.[4c] Luminescence lifetimes were determined on a PRA System 300 time-correlated pulsed single-photon apparatus[19] that is described in detail in an earlier paper.[20] Single exponential decays were observed for each measurement. The reported values represent the average of at least three readings, and the errors for lifetime data were estimated to be less than 10%.

Electrochemical measurements were recorded on a Princeton Applied Research Model 263A potentiostat (EG&G instruments). The electrochemical cell consists of a platinum working electrode, a platinum wire counter electrode, and a $Ag/AgNO_3$ (0.01 M in CH_3CN solution) reference electrode. Cyclic voltammograms were obtained in deoxygenated anhydrous DMF, with the electroactive material (1 mM) and 0.1 M tetrabutylammonium hexafluorophosphate (TBAH) as supporting electrolyte. Ferrocene (Fc) was used as an internal standard for potential calibration, reversibility criteria, and number of electrons exchanged in each redox process.[21] All potentials for the complexes in the study are reported relative to Fc/Fc^+. The scan rate was 200 mV/s, and the measurements were uncorrected for liquid−junction potentials.

General Procedure for Synthesis of the Squares 1 and 2. To a 100 ml flask containing 0.1 mmol of $BrRe(CO)_5$ and 0.1 mmol of $M(pyterpy)_2(PF_6)_2$ was added 20 mL of CH_3CN and 40 ml of THF, successively. The resulting solution was heated to 60 °C for 2 days. The precipitate was collected on frit, washed with THF and diethyl ether, and dried under vacuum to afford an analytical pure product.

Square 1: 91%. IR ($\upsilon_{C\equiv O}$, cm^{-1}, DMSO): 2025, 1927, 1898. ^{1}H NMR (360 MHz, DMSO-d_6): 9.81 (s, 16 H), 9.32 (bd, 16 H), 9.02 (d, 16 H, $J_{H-H} = 7.8$ Hz), 8.43 (bd, 16 H), 8.05 (t, 16 H, $J_{H-H} = 6.9$ Hz), 7.26 (d, 16 H, $J_{H-H} = 5.0$ Hz), 7.19 (t, 16 H, $J_{H-H} = 5.3$ Hz). ^{13}C NMR (DMSO-d_6): 195.9, 191.5, 160.3, 157.5, 155.2, 154.5, 152.8, 151.0, 146.4, 144.7, 139.1, 127.8, 124.5, 121.7. MS *m*/*z*: 1170.8 (calcd 1171.0 for $(M - 4PF_6^-)^{4+}$), 908.1 (calcd 907.8 for $(M - 5PF_6^-)^{5+}$), and 732.4 (calcd 732.3 for $(M - 6PF_6^-)^{6+}$). Anal. Calcd for $C_{172}H_{112}Br_4F_{48}Fe_4N_{32}O_{12}P_8Re_4$: C, 38.23; H, 2.07; N, 8.30. Found: C, 37.87; H, 2.11; N, 8.01.

Square 2: 88%. IR ($\upsilon_{C\equiv O}$, cm^{-1}, CH_3CN): 2028, 1928, 1904. ^{1}H NMR (360 MHz, DMSO-d_6): 9.60 (s, 16 H), 9.11 (d, 16 H, $J_{H-H} = 8.0$ Hz), 8.99 (d, 16 H, $J_{H-H} = 5.9$ Hz), 8.43 (d, 16 H, $J_{H-H} = 6.2$ Hz), 8.09 (t, 16 H, $J_{H-H} = 7.3$ Hz), 7.56 (d, 16 H, $J_{H-H} = 5.1$ Hz), 7.28 (t, 16 H, $J_{H-H} = 7.0$ Hz). ^{13}C NMR (DMSO-d_6): 195.7, 191.2, 161.2, 158.8, 155.8, 154.4, 147.5, 146.7, 141.7, 131.3, 128.4, 125.1, 124.8. MS *m*/*z*: 2578.44 (calcd 2578.90 for $(M - 2PF_6^-)^{2+}$) and 1670.51 (calcd 1670.95 for $(M - 3PF_6^-)^{3+}$). Anal. Calcd for $C_{172}H_{112}Br_4F_{48}N_{32}O_{12}P_8Re_4Ru_4$: C, 37.91; H, 2.06; N, 8.23. Found: C, 37.77; H, 2.25; N, 8.29.

Square 3: The preparation of square **3** was similar to those for squares **1** and **2**. After collecting the precipitate, the solid was purified by column chromatography eluted by a mixture of CH_3CN/saturated aqueous KNO_3/water (8:1:1 v/v). The first brown band is the unreacted $Os(pyterpy)_2$. The second dark purple band is the desired square **3**. The fraction was collected, and a saturated methanolic NH_4PF_6 solution (10 mL) was added. The solution was reduced in volume to precipitate square **3** as the hexafluorophosphate salt. Yield: 78%. IR ($\upsilon_{C\equiv O}$, cm^{-1}, CH_3CN): 2030, 1928, 1904. ^{1}H NMR (360 MHz, DMSO-d_6): 9.61 (s, 16 H), 9.10 (d, 16 H, $J_{H-H} = 7.8$ Hz), 8.99 (d, 16 H, $J_{H-H} = 5.6$

(9) Fujita, M.; Yazaki, J.; Ogura, K. *J. Am. Chem. Soc*. **1990**, *112*, 5645.
(10) Slone, R. V.; Benkstein, K. D.; Bélanger, S.; Hupp, J. T.; Guzei, I. A.; Rheingold, A. L. *Coord. Chem. Rev*. **1998**, *171*, 221.
(11) (a) Rajendran, T.; Manimaran, B.; Lee, F.-Y.; Lee, G.-H.; Peng, S.-M.; Wang, C. M.; Lu, K.-L. *Inorg. Chem*. **2000**, *39*, 2016. (b) Benkstein, K. D.; Hupp, J. T. *Mol. Cryst. Liq. Cryst*. **2000**, *342*, 151. (c) Woessner, S. M.; Helms, J. B.; Houlis, J. F.; Sullivan, B. P. *Inorg. Chem*. **1999**, *38*, 4380. (d) Leadbeater, N. E.; Cruse, H. A. *Inorg. Chem. Commun*. **1999**, *2*, 93. (e) Benkstein, K. D.; Hupp, J. T.; Stern, C. L. *J. Am. Chem. Soc*. **1998**, *120*, 12982. (f) Benkstein, K. D.; Hupp, J. T.; Stern, C. L. *Inorg. Chem*. **1998**, *37*, 5404. (g) Woessner, S. M.; Helms, J. B.; Shen, Y.; Sullivan, B. P. *Inorg. Chem*. **1998**, *37*, 5406. (h) Slone, R. V.; Hupp, J. T.; Stern, C. L.; Albrecht-Schmitt, T. E. *Inorg. Chem*. **1996**, *35*, 4096. (i) Manimaran, B.; Rajendran, T.; Lu, Y.-L.; Lee, G.-H.; Peng, S.-M.; Lu, K.-L. *Eur. J. Inorg. Chem*. **2001**, 633.
(12) (a) Campagna, S.; Denti, G.; Serroni, S.; Ciano, M.; Balzani, V. *Inorg. Chem*. **1991**, *30*, 3728. (b) Denti, G.; Serroni, S.; Campagna, S.; Juris, A.; Ciano, M.; Balzani, V. In *Perspectives in Coordination Chemistry*; Williams, A. F., Floriani, C., Merbach, A. E., Eds; VCH: Basel, 1992; p 153. (c) Chichak, K.; Branda, N. R. *Chem. Commun*. **1999**, 523.
(13) Perrin, D. D.; Armarego, W. L. F. *Purification of Laboratory Chemicals*, 3rd ed.; Pergamon Press: Oxford, U. K., 1988.
(14) (a) Constable, E. C.; Cargill Thompson, A. M. W. *J. Chem. Soc., Dalton Trans*. **1992**, 2947. (b) Hathcock, D. J.; Stone, K.; Madden, J.; Slattery, S. J. *Inorg. Chim. Acta* **1998**, *282*, 131.
(15) Constable, E. C.; Cargill Thompson, A. M. W. *J. Chem. Soc., Dalton Trans*. **1994**, 1409.
(16) Stang, P. J.; Olenyuk, B.; Fan, J.; Arif, A. M. *Organometallics* **1996**, *15*, 904.
(17) Kober, E. M.; Caspar, J. V.; Lumpkin, R. S.; Meyer, T. J. *J. Phys. Chem*. **1986**, *90*, 3722.
(18) Demas, J. N.; Crosby, G. A. *J. Phys. Chem*. **1971**, *75*, 991.
(19) O'Connor, D. V.; Phillips, D. *Time-Correlated Single Photon Counting*; Academic: London, 1984.
(20) (a) Wang, Z.; Lees, A. J. *Inorg. Chem*. **1993**, *32*, 1493. (b) Zulu, M. M.; Lees, A. J. *Inorg. Chem*. **1988**, *27*, 1139.
(21) Gritzner, G.; Kuta, J. *Pure Appl. Chem*. **1984**, *56*, 461.

Scheme 1

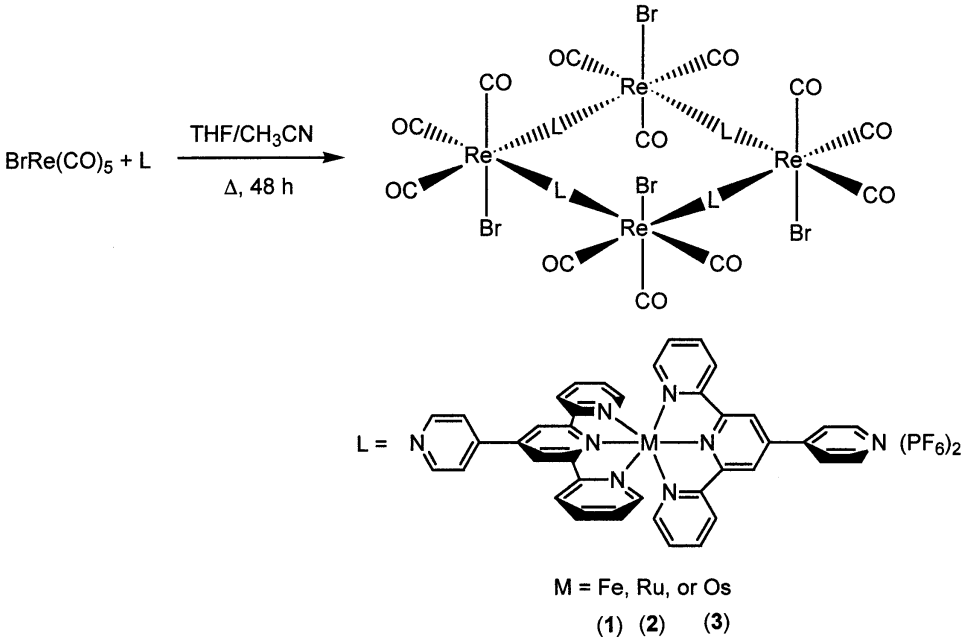

Hz), 8.42 (d, 16 H, J_{H-H} = 5.5 Hz), 7.95 (t, 16 H, J_{H-H} = 6.3 Hz), 7.44 (d, 16 H, J_{H-H} = 5.5 Hz), 7.22 (t, 16 H, J_{H-H} = 6.4 Hz). The solubility of square **3** in DMSO-d_6 or other polar solvents is too low to obtain well-resolved ^{13}C spectra. MS *m*/*z*: 1307.0 (calcd. 1307.0 for $(M - 4\ PF_6^-)^{4+}$). Anal. Calcd for $C_{172}H_{112}Br_4F_{48}N_{32}O_{12}P_8Re_4Os_4$: C, 35.59; H, 1.95; N, 7.72. Found: C, 35.29; H, 2.16; N, 8.02.

Square 4: To a 25 ml flask containing 0.1 mmol of $(dppf)Pd(H_2O)_2(OTf)_2$ and 0.1 mmol of $Ru(pyterpy)_2(PF_6)_2$ was added 10 ml of CH_3NO_2 under nitrogen. The mixture was refluxed for 2 h. Subsequently, the CH_3NO_2 solution was transferred to a 250 ml flask containing 200 ml of rapid stirring cold diethyl ether. The resulting precipitate was collected on frit, washed with diethyl ether, and dried under vacuum to afford the analytical pure product. Yield: 95%. ^{1}H NMR (300 MHz, CD_3CN): 8.97 (s, 16 H), 8.86 (bd, 16 H,), 8.66 (d, 16 H, J_{H-H} = 7.9 Hz), 8.11 (bd, 16 H), 7.94−7.65 (m, 96 H), 7.39 (bd, 16 H), 7.18 (bt, 16 H), 4.77 (bd, 16 H, J_{H-P} = 87.3 Hz), 3.41 (d, 16 H, J_{H-H} = 6.8 Hz). ^{13}C NMR (CD_3CN): 159.1, 157.2, 153.9, 151.7, 148.4, 145.2, 139.7, 135.5 (d, J_{C-P} = 11.4 Hz), 134.8, 133.8, 131.2 (d, J_{C-P} = 11.4 Hz), 129.7, 129.2, 126.3, 125.4, 123.3, 120.4, 79.2, 77.6, 75.9. ^{31}P NMR (CD_3CN): 38.7 (s), −142.9 (heptet, J_{P-F} = 699 Hz). ^{19}F NMR (CD_3CN): −70.5 (d, J_{F-P} = 711 Hz), −80.3 (s). MS *m*/*z*: 1821.5 (calcd 1821.0 for $(M - 4\ OTf^-)^{4+}$) and 1170.3 (calcd 1168.4 for $(M - 6\ PF_6^-)^{6+}$). Anal. Calcd for $C_{304}H_{224}F_{72}N_{32}O_{24}P_{16}S_8Fe_4Pd_4Ru_4$: C, 46.32; H, 2.86; N, 5.69. Found: C, 46.69; H, 3.11; N, 5.63.

***fac*-BrRe(CO)$_3$(pyterpy)$_2$ (5):** Square **1** (60 mg, 0.011 mmol) was suspended in 100 ml of water and acetonitrile mixture (1:1 in volume) containing 0.2 g of NaOH. The solution was added dropwise to 30% H_2O_2 until the purple color disappeared. The brown solution was filtered, and the filtrate was extracted with CH_2Cl_2 (3 × 50 mL) and dried over $MgSO_4$. The solvent was removed, and the brown solid obtained was subjected to column chromatography on neutral alumina. The first band was eluted by CH_3CN/toluene (1:1) to afford orange powdery **5** (10 mg, 23%). IR ($\upsilon_{C\equiv O}$, cm^{-1}, CH_2Cl_2): 2026, 1926, 1898. ^{1}H NMR (300 MHz, acetone-d_6): 9.14 (d, 4 H, J_{H-H} = 6.7 Hz), 8.88 (s, 4 H), 8.74−8.72 (m, 8 H), 8.15 (d, 4 H, J_{H-H} = 6.8 Hz), 8.01 (t, 4 H, J_{H-H} = 7.6 Hz), 7.49 (t, 16 H, J_{H-H} = 7.7 Hz). Anal. Calcd for $BrC_{43}H_{28}N_8O_3Re$: C, 53.20; H, 2.91; N, 11.54. Found: C, 53.15; H, 2.88; N, 11.43.

Results and Discussion

Preparation and Characterization. Squares **1**−**3** were prepared by reaction between $BrRe(CO)_5$ and the metal-complex bridging ligands in refluxing CH_3CN/THF mixture (see Scheme 1). Square **4** was prepared by reaction between $(dppf)Pd(H_2O)_2(OTf)_2$ and $(pyterpy)_2Ru(PF_6)_2$ in CH_3NO_2 solution (see Scheme 2). The corner complex **5** was prepared in low yield by removing the iron atoms from square **1** following a literature procedure (see Scheme 3).[22] In each of the squares **1**−**3**, four possible diastereomers with respect to the relative positions of CO and Br^- may exist.[10h] In Scheme 1, we do not intend to specify any isomer that is preferentially formed during the self-assembly process. A variety of analytical methods were employed to characterize the square structures, and all obtained data confirm the 1:1 stoichiometry between the corner component (*fac*-$BrRe(CO)_3$ or *cis*-(dppf)Pd) and the metal-complex bridging ligand. The clean and sharp peaks in the ^{1}H NMR spectra indicate that a single species is present in the solution and exclude the possibility of formation of polymeric or oligomeric species in each case. In general, the peaks in ^{1}H NMR are all downfield shifted in squares **1**−**3** when compared to their corresponding metal-complex bridging ligands. However, the protons are slightly upfield shifted in square **4** (0.03, 0.11, and 0.10 ppm for H_α, H_β, and $H_{3'}$, respectively, see Chart 1 for proton labeling) in comparison to the protons in $Ru(pyterpy)_2(PF_6)_2$. The less downfield shifting of H_α than H_β may be due to the ring current effect generated from the phenyl groups in dppf. The downfield shifting for H_α, H_β, and $H_{3'}$ indicates that the electron-donating dppf renders the (dppf)Pd(II) moiety less acidic compared to $Br(CO)_3Re(I)$. The subtle difference in the electron accepting abilities of (dppf)Pd(II) and $Br(CO)_3Re(I)$ also results in a slight difference in the band positions of the electronic absorption spectra for these square complexes (vide infra). The ^{31}P NMR spectrum of square **4** shows two signals, one singlet at 38.7 ppm and one heptet at −142.9 ppm. The singlet corresponds to the phosphorus in dppf, and the heptet originates from the PF_6^- counteranion. The appearance of a single ^{31}P signal from dppf indicates that square **4** has a highly symmetric structure. Several attempts have been made to obtain X-ray quality crystals and, while we found it possible to grow very small crystals from slow diffusion of ether into CH_3CN/

(22) (a) Constable, E. C.; Ward, M. D. *Inorg. Chim. Acta* **1988**, *141*, 201. (b) Constable, E. C.; Cargill Thompson, A. M. W.; Tocher, D. A.; Daniels, M. A. M. *New J. Chem.* **1992**, *16*, 855.

Scheme 2

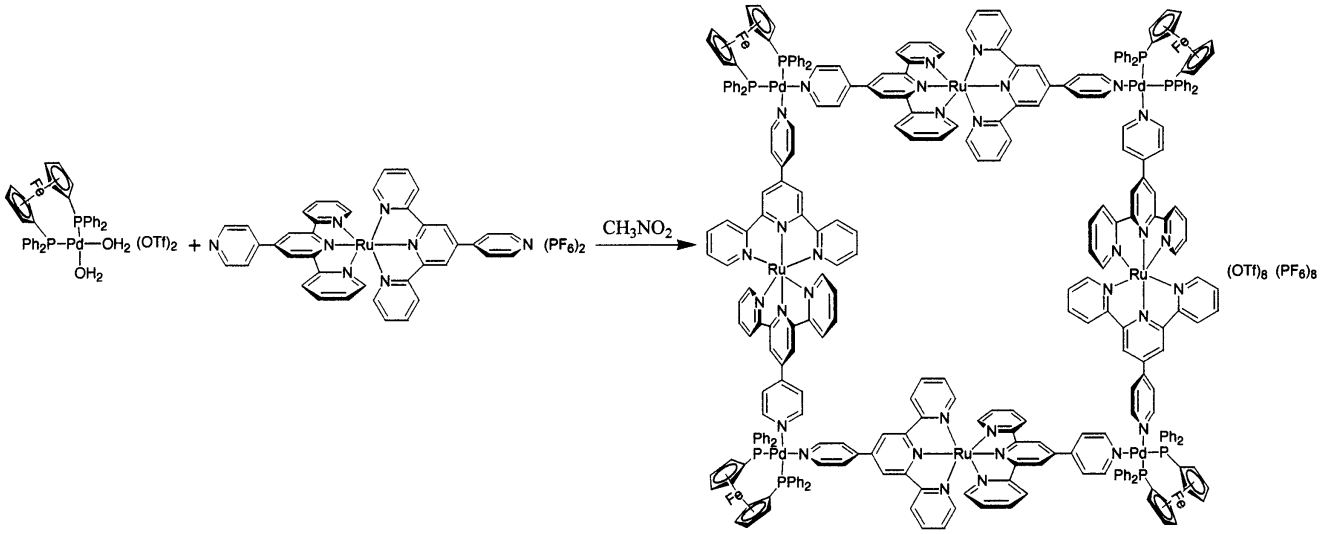

(4)

Scheme 3

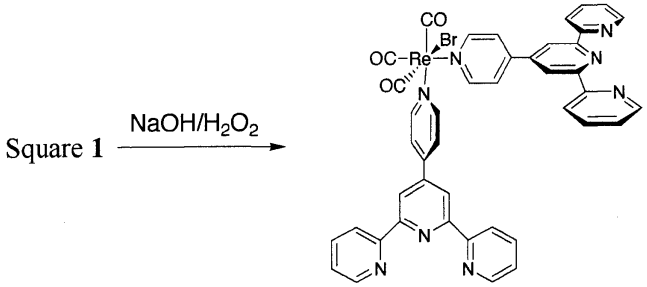

(5)

Chart 1

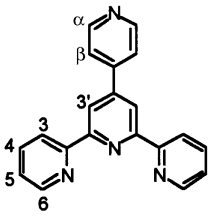

DMSO solution, these crystals underwent solvent loss readily and collapsed to form amorphous solids immediately after they were removed from the mother liquor.

We have obtained direct evidence for the square structures of compounds **1**−**4** from electrospray ionization (ESI) mass spectra. Electrospray ionization mass spectrometry (ESI-MS) has been successfully used for detection of supramolecular species in solution.[23] The efficient ionization process and the multiple-charging phenomenon inherent in ESI mass spectra have provided high sensitivities and the observation of high molecular weight species within a limited mass-to-charge ratio observation window. On gentle ionization, even highly charged intact species can be observed without undergoing fragmentation.[23a,24] We have recorded a high-resolution ESI mass spectrum for complex **2** utilizing the Fourier transform ion cyclotron resonance (FTICR) technique. Figure 1 illustrates the ESI−FTICR mass spectrum and the calculated and experimental isotopic distribution for complex **2** based on $[\mathbf{2} - 2\ PF_6^-]^{2+}$, and the excellent agreement between the calculated and experimental isotopic pattern clearly confirms the square structure. Several literature reports have suggested the coexistence of molecular triangle and square structures in solution and, indeed, other physical data (IR, NMR, and elemental analysis) for such species ought to be very similar.[25] However, there is no indication of a molecular weight in any of the mass spectra that corresponds to either the molecular triangle or other higher order structures. The exceptionally clean NMR spectra are also evidence for a single product in the self-assembly process.

The sizes of squares **1**−**4**, based on MM3 molecular modeling and defined by interatomic distances between Re−Re or Pd−Pd, are 21.8 × 21.7 Å (**1**), 21.9 × 21.8 Å (**2**), 21.9 × 21.8 Å (**3**), and 21.8 × 21.8 Å (**4**).[26] Thus, squares **1**−**4** represent some of the largest self-assembly molecular squares reported in the literature. However, the effective internal cavities for these squares are much smaller than measurements from the edges due to the perpendicular arrangement of two terpyridine units around the center metals.

Electrochemical Properties. Cyclic voltammetric experiments were performed in deoxygenated DMF solution; in several cases, DMF has proven to be a superior solvent for studying

(23) (a) Olenyuk, B.; Whiteford, J. A.; Fechtenkotter, A.; Stang, P. J. *Nature* **1999**, *398*, 796. (b) Przybylski, M.; Glocker, M. O. *Angew. Chem., Int. Ed. Engl.* **1996**, *35*, 806 and references therein. (c) Marquis-Rigault, A.; Dupont-Gervais, A.; Baxter, P. N. W.; Van Dorsselaer, A.; Lehn, J.-M. *Inorg. Chem.* **1996**, *35*, 2307. (d) Fujita, M.; Nagao, S.; Ogura, K. *J. Am. Chem. Soc.* **1995**, *117*, 1649. (e) Leize, E.; Van Dorsselaer, A.; Kramer, R.; Lehn, J.-M. *J. Chem. Soc., Chem. Commun.* **1993**, 990. (f) Bitsch, F.; Dietrich-Buchecker, C. O.; Khémiss, A.-K.; Sauvage, J.-P.; Van Dorsselaer, A. *J. Am. Chem. Soc.* **1991**, *113*, 4023.

(24) (a) Constable, E. C.; Schofield, E. *Chem. Commun.* **1998**, 403. (b) Manna, J.; Kuehl, C. J.; Whiteford, J. A.; Stang, P. J.; Muddiman, D. C.; Hofstadler, S. A.; Smith, R. D. *J. Am. Chem. Soc.* **1997**, *119*, 11611. (c) Manna, J.; Whiteford, J. A.; Stang, P. J.; Muddiman, D. C.; Smith, R. D. *J. Am. Chem. Soc.* **1996**, *118*, 8731.

(25) (a) Cotton, F. A.; Daniel, L. M.; Lin, C.; Murillo, C. A. *J. Am. Chem. Soc.* **1999**, *121*, 4538. (b) Cotton, F. A.; Daniels, L. M.; Lin, C.; Murillo, C. A. *Chem. Commun.* **1999**, 841. (c) Lee, S. B.; Hwang, S.; Chung, D. S.; Yun, H.; Hong, J.-I. *Tetrahedron Lett.* **1998**, *39*, 873. (d) Baxter, P. N. W.; Lehn, J. -M.; Rissanen, K. *Chem. Commun.* **1997**, 1323. (e) Fujita, M.; Sasaki, O.; Mitsuhashi, T.; Fujita, T.; Yazaki, J.; Yamaguchi, K.; Ogura, K. *Chem. Commun.* **1996**, 1535.

(26) CAChe 4.5 for Power Macintosh, Fujitsu Limited, 2000.

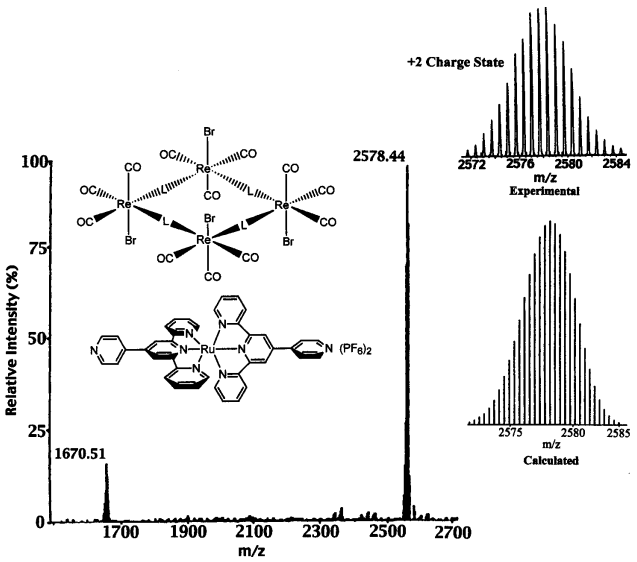

Figure 1. ESI−FTICR mass spectrum of square **2**.

Table 1. Redox Potentials[a]

compounds	E_{ox}, V[b]	E_{red}, V
1	0.65	−1.41, −1.54
2	0.76	−1.51, −1.83
3	0.48	−1.54, −1.84
4	0.70, 0.88	−1.61, −1.89
5	*b*	−1.69 (i)
$(pyterpy)_2Fe(PF_6)_2$	0.55	−1.58, −1.70
$(pyterpy)_2Ru(PF_6)_2$	0.70	−1.59, −1.85
$(pyterpy)_2Os(PF_6)_2$	0.45	−1.58, −1.86
$(dppf)Pd(4\text{-}phpy)_2(OTf)_2$[c]	0.81	−1.75 (i), −2.07 (i)
pyterpy		−2.24

[a] Analyses were performed in 1 mM deoxygenated DMF solutions containing 0.1 M TBAH, scan rate is 200 mV/s. All potentials in volts versus $[Fe(C_5H_5)_2]^{+/0}$ (0.13 V with peak separation 78 mV in DMF); (i) = irreversible process. [b] The oxidation potentials of Re(+1/+2) are out of the solvent window. [c] 4-phpy is 4-phenylpyridine.

multiple reduction processes in cyclic voltammetry.[27] The obtained redox potentials are summarized in Table 1. For each of the four square complexes, a reversible oxidation wave was observed for $M^{+2/+3}$ (M = Fe, Ru, or Os), and an additional irreversible oxidation wave that appears at higher potential for square **4** is assigned to $Fc^{+1/+2}$. The oxidation potentials for $Re^{1+/2+}$ are out of the solvent window and are not observed in squares **1**−**3** and corner **5**. All oxidation potentials obtained for squares **1**−**4** exhibit multielectron processes, ca. 4 e^-, based on the current intensity using ferrocene as the internal reference. The appearance of simultaneous electron transfer indicates that there is negligible communication between the metal centers.[28] All square complexes exhibit two reductions which are assigned to pyterpy-based reductions. The reduction potentials also exhibit multielectron-transfer processes similar to the oxidation processes.

It is interesting to compare the redox potentials between square complexes and their corresponding metal-complex ligands. Except for square **4**, the oxidation potentials localized on the metal-complex ligands in the square complexes are anodically shifted compared to their corresponding free metal-complex ligands; this is understood to be due to the dative bonding character of the ligands. The degree of anodic shift is in the order of square **1** (100 mV) > square **2** (60 mV) > square **3** (30 mV). The anodic shift indicates that the electron-withdrawing $BrRe(CO)_3$ moiety destabilizes the metal with respect to oxidation to a M^{+3} state. In the case of square **4**, there is virtually no shift of the oxidation potential $Ru^{2+/3+}$ because of the electron donating dppf ligand, which compensates the electron density loss on the bridging metal-complex during the coordination.

Squares **1** (170 mV), **2** (80 mV), and **3** (40 mV) also exhibit a significant anodic shift in their first reduction potential compared to their metal-complex ligands. The overall effect of coordination to the corner metals ($BrRe(CO)_3$ or (dppf)Pd) is the reduction of the energy gap between the d orbital localized on central metal and π^* orbital localized on pyterpy, in other words, the energy of the MLCT levels. Consequently, the cyclic voltammetry data agree well with the electronic absorption spectral data (vide infra).

Photophysical Properties. Electronic absorption and luminescence data recorded from the squares **1**−**4**, corner **5**, metal-complex bridging ligands, and pyterpy are summarized in Table 2. Figure 2 shows the absorption spectra of squares **1**−**4**. All four squares display broad and intense visible absorptions in the region 400−600 nm, which are assigned to metal (Fe, Ru, or Os)-to-ligand (pyterpy) charge transfer (MLCT) bands.[15] Square **3** exhibits an additional weak band at 676 nm, which is assigned to an Os-based ^{3}MLCT (Os-^{3}MLCT) band.[15,31] For each complex, the bands centered between 279 and 377 nm are assigned to pyterpy-based $\pi-\pi^*$ bands and the Re-based MLCT band on consideration of the absorption spectra of pyterpy and corner **5**. The formation of Re(I)-based square complexes shifts the MLCT band to lower energy as compared to their metal-complex bridging ligands. Coordination of the free 4-pyridyl ring in the metal-complex ligand to the Re(I) center lowers the π^* orbital localized on pyterpy and, thus, red shifts the corresponding MLCT band. Similar red-shift behaviors have also been observed when these metal-complex ligands are protonated or methylated in the 4-pyridyl positions.[15]

An alternative explanation for the red shift is the more extended conjugation in square complexes compared to the free bridging ligands. However, in view of the noninteracting redox potentials (vide supra), such a possibility is less likely. For squares **1** and **2**, the MLCT band red shifts 599 and 412 cm^{-1} relative to $(pyterpy)_2Fe(PF_6)_2$ and $(pyterpy)_2Ru(PF_6)_2$, respectively. The red shifting of the MLCT bands in square **3** is less prominent; the ^{1}MLCT band is 168 cm^{-1} red-shifted and the ^{3}MLCT band is red-shifted 177 cm^{-1} compared to the corresponding MLCT bands in $(pyterpy)_2Os(PF_6)_2$. In the case of square **4**, the Ru(II)-to-pyterpy MLCT band does not shift in comparison to the MLCT band in $(pyterpy)_2Ru(PF_6)_2$. The electron-donating dppf ligand certainly plays an important role here as it reduces the electron-accepting ability in Pd(II).

Squares **1**, **2**, and **4** do not have any detectable solution luminescence at room temperature, even though both the pyterpy ligand and the corner **5** emit in room-temperature solution. The

(27) (a) Ruben, M.; Breuning, E.; Gisselbrecht, J.-P.; Lehn, J.-M. *Angew. Chem., Int. Ed.* **2000**, *39*, 4139. (b) Hartmann, H.; Berger, S.; Winter, R.; Fiedler, J.; Kaim, W. *Inorg. Chem.* **2000**, *39*, 4977. (c) Marcaccio, M.; Paolucci, F.; Paradisi, C.; Roffia, S.; Fontanesi, C.; Yellowless, L. J.; Serroni, S.; Campagna, S.; Denti, G.; Balzani, V. *J. Am. Chem. Soc.* **1999**, *121*, 10081. (d) Fees, J.; Kaim, W.; Moscherosch, M.; Matheis, W.; Klima, J.; Krejcik, M.; Zalis, S. *Inorg. Chem.* **1993**, *32*, 166.

(28) Flanagan, J. B.; Margel, S.; Bard, A. J.; Anson, F. C. *J. Am. Chem. Soc.* **1978**, *100*, 4248.

(29) Tapolsky, G.; Duesing, R.; Meyer, T. J. *Inorg. Chem.* **1990**, *29*, 2285.

(30) Morris, J. V.; Mahaney, M. A.; Huber, J. R. *J. Phys. Chem.* **1976**, *80*, 969.

(31) Campagna, S.; Denti, G.; Sabatino, L.; Serroni, S.; Ciano, M.; Balzani, V. *J. Chem. Soc., Chem. Commun.* **1989**, 1500.

Table 2. Electronic Absorption and Emission Spectra at 293 K

compounds	λ_{max}, nm (ϵ x 10^{-3}, $M^{-1}cm^{-1}$)	λ_{em}, nm	τ, ns	Φ_{em}[a]
1[b]	281 (279), 333 (200), 345 (192), 377 (107), 588 (147)	c		
2[b]	279 (278), 320 (175), 332 (159), 498 (133)	c		
3[d,e]	238 (196), 275 (281), 318 (222), 402 (49.4), 490 (122), 676 (30.9)	748	42	4.2×10^{-4}
4[d]	236 (242), 275 (327), 313 (251), 331 (181), 488 (115)	c		
5[d,f]	244 (80.9), 274 (62.8), 317 (33.0), 379 (sh, 6.55)	530	646	1.8×10^{-3}
$(pyterpy)_2Fe(PF_6)_2$[d]	245 (62.9), 276 (93.8), 283 (102), 324 (60.8), 334 (55.5), 374 (9.2), 568 (34.2)	c		
$(pyterpy)_2Ru(PF_6)_2$[d]	240 (58.9), 276 (95.0), 313 (61.1), 333 (48.5), 488 (36.3)	c		
$(pyterpy)_2Os(PF_6)_2$[d,e]	239 (48.4), 276 (68.3), 317 (56.3), 394 (11.1), 486 (27.3), 668 (7.1)	740	67	6.7×10^{-4}
pyterpy[g]	244 (38.5), 279 (26.2), 315 (8.8)	359	1.4	7.0×10^{-2}

[a] Quantum yield is calculated relative to $Os(bpy)_3(PF_6)_2$ in CH_3CN, unless otherwise stated.[16] [b] DMSO solution. [c] No luminescence detected. [d] CH_3CN solution. [e] $\lambda_{ex} = 490$ nm. [f] $\lambda_{ex} = 380$ nm. Quantum yield is calculated relative to $[(bpy)Re(CO)_3(4\text{-}Etpy)](PF_6)$ ($\Phi_{em} = 0.027$ in CH_3CN).[29] [g] CH_2Cl_2 solution, $\lambda_{ex} = 320$ nm. Quantum yield is calculated relative to 9,10-diphenylanthracene ($\Phi_{em} = 0.95$ in EtOH).[30]

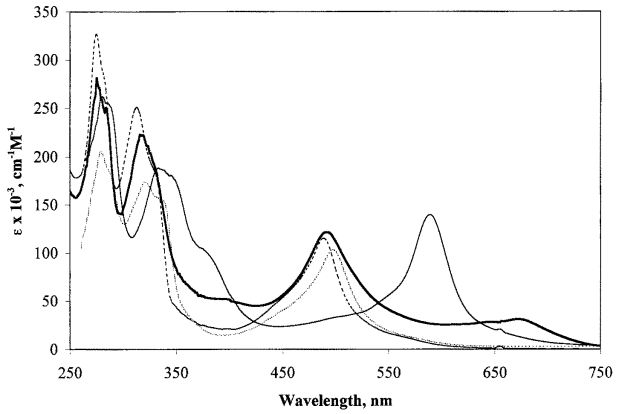

Figure 2. Electronic absorption spectra of squares **1**−**4** in DMSO (squares **1** (solid line) and **2** (thin dash line)) or CH_3CN (squares **3** (thick solid line) and **4** (dashed line)) at 293 K.

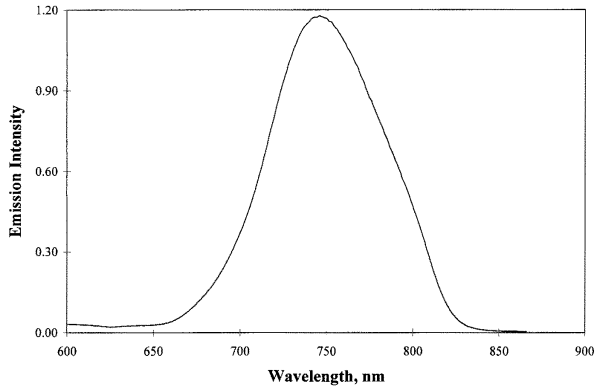

Figure 3. Emission spectrum of square **3** in deoxygenated CH_3CN solution at 293 K.

corner **5** exhibits luminescence at 538 nm in CH_3CN with a lifetime of 646 ns, which is typical of ^{3}MLCT emission. Pyterpy emits at 359 nm in CH_2Cl_2 with a lifetime of 1.4 ns. The small Stokes shift and very short lifetime indicate that the emission originates from a singlet $\pi-\pi^*$ excited state. The lack of luminescence at room temperature from squares **1**, **2**, and **4** is attributed to the existence of metal-centered (MC) states lying in close proximity to the MLCT states. The distortion from perfect octahedral structure, due to the C_{2v} symmetry in $M(pyterpy)_2$ (M = Fe, Ru), results in a relatively weak ligand field at the metal and, thus, the MC states are at low energy.[32] The MLCT excited states appear to be deactivated through these low-lying nonemissive MC states via an efficient nonradiative decay pathway. The low-lying MC states localized in ferrocenyl moieties in square **4** also provide an additional radiationless relaxation pathway for the deactivation of the MLCT excited states.[33]

In contrast, square **3** exhibits room-temperature luminescence in deoxygenated CH_3CN solution (see Figure 3). The origin of the emission is assigned to a Os(II)-based ^{3}MLCT transition. The stronger ligand field and lower oxidation potential of Os(II) compared to Ru(II) and Fe(II) results in an increased energy gap between the ^{3}MLCT and ^{3}MC states.[1a] Therefore, it can be inferred that the ^{3}MC excited states are not so readily thermally populated in square **3**. The luminescence of square **3** exhibits a lower energy emission feature with a shorter lifetime and lower quantum yield compared to $(pyterpy)_2Os(PF_6)_2$ (Table 2). This observation is in accordance with the energy gap law and is a consequence of the more efficient nonradiative decay in square **3** than in $(pyterpy)_2Os(PF_6)_2$.[17] The quantum yield and position of emission of square **3** is also independent of the excitation wavelength, and excitation of square **3** at 380 nm, where the Re(I) moiety is the sole chromophore, results in a luminescence band centered at 676 nm. The same luminescence position is also observed when square **3** is excited at 490 nm. The wavelength independent luminescence band implies that the energy transfer from higher energy states (Re MLCT or $\pi-\pi^*$) to the lowest Os ^{3}MLCT state is very efficient and close to unity.

Figure 4 illustrates the spectral overlap between the absorption band of square **3** and the emission feature of corner **5**. The spectral overlap occurs from the red edge of the singlet absorption band to the triplet absorption band. Thus, it can be concluded that the intramolecular energy transfer is most likely to be a triplet−triplet process. The complete quenching of the emission from the Re(I)-based donor in square **3** indicates that

(32) (a) Indelli, M. T.; Scandola, F.; Flamigni, L.; Collin, J.-P.; Sauvage, J.-P.; Sour, A. *Inorg. Chem.* **1997**, *36*, 4247. (b) Calvert, J. M.; Caspar, J. V.; Binstead, R. A.; Westmoreland, T. D.; Meyer, T. J. *J. Am. Chem. Soc.* **1982**, *104*, 6620.
(33) Lee, E. J.; Wrighton, M. S. *J. Am. Chem. Soc.* **1991**, *113*, 8562.

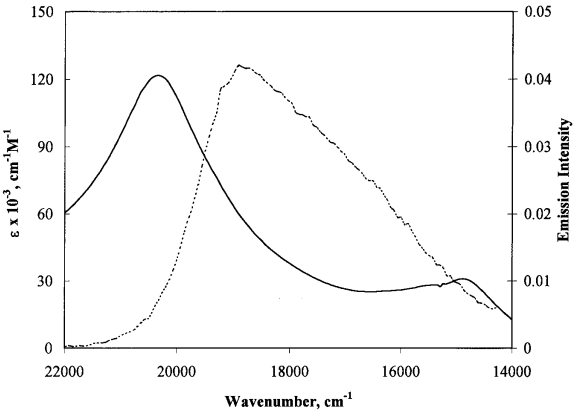

Figure 4. Spectral overlap between absorption spectrum of square **3** (solid line) and emission spectrum of corner **5** (dashed line) in deoxygenated CH_3CN solution.

the energy transfer rate is much faster than 1×10^{10} s^{-1}.[34] The Re(I) to Os(II) separation and the distance between the edges of the coordinating ligands are 10.9 and 1.5 Å, respectively. Given that there is a such short distance of separation between the Re(I) donor and Os(II) acceptor and a large degree of triplet character involved, it can be concluded that the energy transfer occurs likely via a Dexter-type electron exchange process,[35] although the participation of a Förster-type dipole−dipole mechanism cannot be completely ruled out.[36] A qualitative energy level diagram of square **3** is summarized in Scheme 4, depicting the energy levels and processes of the Re- and Os-based moieties.

The highly positive charges and luminescent behavior of square **3** have prompted us to study its potential use as a host for inorganic anionic species.[5e,10] We have tested several inorganic polyatomic anions, such as BF_4^-, CH_3COO^-, PF_6^-, and OTf^-, with the expectation of observing changes in luminescence intensities that arise from host−guest interactions. Unfortunately, in this particular square molecule, we have found that the emission results are irreproducible, and we noted that decomposition of square **3** was usually observed when excess anions were added into the solution containing this complex. The large internal cavity of square **3**, which minimizes the electrostatic and/or any hydrophobic interactions between square **3** and guest anions, and the difference in stability provided by counterions may account for the square decomposition and the irreproducibility of the results.

Scheme 4

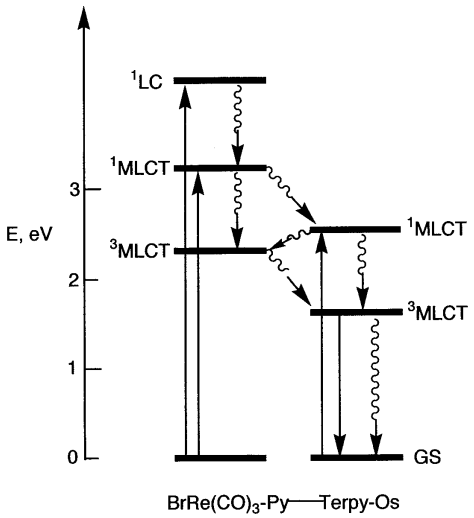

Conclusion

We have demonstrated here that metal complexes with pendant pyridines can be used as linear bridging ligands for the construction of large square structures in a self-assembly manner. The dimensions of these large squares are about 21.8 × 21.8 Å, which represent some of the largest molecular squares reported in the literature to date. All square complexes exhibit multielectron redox processes, indicating a negligible electronic communications between the individual chromophores. The observed photophysical properties are dominated by the bridging metal-complex ligands with minimum influence from the corner chromophores.

Acknowledgment. We are grateful to the Division of Chemical Sciences, Office of Basic Energy Sciences, Office of Science, U. S. Department of Energy (Grant DE-FG02-89ER14039) for support of this research. Prof. Omowunmi A. Sadik and Prof. Wayne E. Jones are thanked for the use of electrochemical apparatus. We also thank Ms. Alexsandra S. Silva for some preliminary photophysical measurements on square **3** and Dr. Jürgen Schulte for helping to acquire ^{31}P and ^{19}F NMR spectra.

IC0101681

(34) (a) Grosshenny, V.; Harriman, A.; Ziessel, R. *Angew. Chem., Int. Ed. Engl*. **1995**, *34*, 1100. (b) Grosshenny, V.; Harriman, A.; Hissler, M.; Ziessel, R. *J. Chem. Soc., Faraday Trans*. **1996**, *92*, 2223.

(35) (a) Dexter, D. L. *J. Chem. Phys*. **1953**, *21*, 836. (b) Levy, S. T.; Rubin, M. B.; Speiser, S. *J. Am. Chem. Soc*. **1992**, *114*, 10747. (c) Levy, S. T.; Rubin, M. B.; Speiser, S. *J. Chem. Phys*. **1992**, *96*, 3585.

(36) Förster, T. *Discuss. Faraday Soc*. **1959**, *27*, 7.